



ELSEVIER

Earth and Planetary Science Letters 146 (1997) 315–327

EPSL

# The cosmochemical behavior of beryllium and boron

Dante S. Lauretta<sup>\*</sup>, Katharina Lodders

*Planetary Chemistry Laboratory, Department of Earth and Planetary Sciences, Campus Box 1169, Washington University, One Brookings Drive, St. Louis, MO 63130-4899, USA*

Received 10 July 1996; accepted 24 October 1996

## Abstract

The chemistry of Be and B in the solar nebula is reinvestigated using thermodynamic equilibrium calculations. The dominant Be gases are monatomic Be at high temperatures and the hydroxides BeOH and Be(OH)<sub>2</sub> at lower temperatures. Beryllium condenses as gugiaite (Ca<sub>2</sub>BeSi<sub>2</sub>O<sub>7</sub>) in solid solution with melilite with a 50% condensation temperature of 1490 K. If an ideal solid solution of chrysoberyl (BeAl<sub>2</sub>O<sub>4</sub>) into spinel is assumed, most of the Be condenses into spinel, yielding a 50% condensation temperature of 1501 K. However, the difference in the crystal structures of spinel and chrysoberyl indicates that their solid solution may be non-ideal. At high temperatures the dominant B gases are BO, HBO, and HBO<sub>2</sub>, while NaBO<sub>2</sub>, KBO<sub>2</sub>, and LiBO<sub>2</sub> are dominant at lower temperatures. Boron is less refractory than Be and is calculated to condense into solid solution with feldspar. The majority of B condenses as danburite (CaB<sub>2</sub>Si<sub>2</sub>O<sub>8</sub>) in solid solution with anorthite. At lower temperatures, when the feldspar composition is more albitic, the remaining B condenses as reedmergnerite (NaBSi<sub>3</sub>O<sub>8</sub>). The 50% condensation temperature of B is 964 K. The 50% condensation temperature of B is similar to that of Na and much higher than that of S. Therefore, normalized B abundances in chondrites are expected to correlate with Na abundances. Be is predicted to be concentrated in melilite, a conclusion which is consistent with the few measurements of Be concentrations in calcium aluminum-rich inclusions (CAIs). Boron is predicted to be concentrated in feldspar, but no analytical data are available to test this prediction.

*Keywords:* condensation; solar nebula; beryllium; boron

## 1. Introduction

Generally, the elemental abundances in CI chondrites match those in the solar photosphere [1]. As a result, elemental abundances in CI chondrites are generally taken as equivalent to solar elemental abundances. However, there are several groups of elements for which this is not true. One group of

elements whose meteoritic and solar abundances do not correlate are the atmophile elements (H, C, N, O and the noble gases). These elements are depleted in chondrites due to incomplete condensation in the solar nebula. A second group of elements for which the correlation does not hold are light elements (Li, Be and B), which are more abundant in CI chondrites than in the solar photosphere. Lithium, Be, and B are assumed to have fully condensed into solid material during the early history of the solar system. These light element nuclei are unstable at the high temperatures found in stellar interiors and, instead of

<sup>\*</sup> Corresponding author. Tel: +1 314 935 4851. Fax: +1 314 935 4853. E-mail: lauretta@wunder.wustl.edu

being created, these elements are destroyed during ongoing nucleosynthetic processes in the sun [2]. Therefore, the meteoritic abundances of these elements are thought to represent their initial solar system abundance.

Since the light elements are not created in stellar interiors like most other elements, different production mechanisms are responsible for their existence. Hydrogen, He, and some Li nuclei are thought to have formed during the “Big Bang” [3]. Several formation mechanisms have been proposed for both Be and B. Some models propose the formation of Be and B on the surface of flaring stars [4,5] and during supernova-driven reactions [6]. Currently, models proposing that Be and B nuclei result from collisions between heavier nuclei (C and O) and galactic cosmic rays are the most widely accepted [7,8]. Each model makes specific predictions about the relative abundance and isotopic composition of Be and B.

In order to test these models, independent measurements of the Be and B abundances and their isotopic ratios in solar system material must be made. In principle, the Be and B abundances and isotopic ratios in the atmosphere of Jupiter could be used but these data are unknown. Models of Jovian atmospheric chemistry predict that all B and Be will condense deep in Jupiter’s atmosphere [9]. In addition, the preliminary results of the Galileo mass spectrometer experiment indicate that heavy elements (except neon and oxygen) are enriched relative to solar composition in Jupiter’s atmosphere [10]. Thus, the only place where the nebular abundances of Be and B are recorded is in primitive chondrites. Unfortunately, the low abundance of Be and B and the high probability of laboratory contamination make these measurements difficult, requiring sensitive techniques [11]. Often, only the bulk abundance of Be and B in meteorites is determined. More precise data about the relative abundance and isotopic composition of Be and B could be obtained from the composition of mineral grains having large concentrations of these elements. In order to determine which meteoritic minerals would contain the largest concentration of these elements we performed condensation calculations for known Be and B minerals. These calculations provide information about the distribution of Be and B between gaseous and solid phases in the solar nebula as a function of

temperature. This information is important for understanding the overall chemical behavior of the early solar system.

## 2. Previous condensation calculations

The most important quantities needed to calculate the condensation behavior of an element are its total nebular abundance, the gas pressure of the nebula, and the thermodynamic properties for all possible compounds. Variations in any of these quantities can alter the condensation temperature.

Since Li, Be and B all share a common origin [3–8], it is useful to determine the cosmochemical behavior of these three elements together. The condensation of Li was investigated by Wai and Wasson [12]. They determined that the major gaseous form of Li is Li(g) and that Li condenses as  $\text{Li}_2\text{SiO}_3$  in solid solution with enstatite yielding a 50% condensation temperature of 1225 K at  $10^{-4}$  bar total nebular pressure.

Previous determinations of condensation temperatures for Be and B are summarized in Table 1. These values span an unsatisfactorily large range. Previous estimates of the Be condensation temperature range from 980 to 1400 K while results for B range from 400 to 1200 K. For comparison, our results are also shown in Table 1.

The first condensation calculations for Be and B were made by Cameron et al. [13], who calculated that B condenses as pure  $\text{NaBO}_2$  at a temperature of  $\sim 750$  K, a pressure of  $10^{-3}$  bar, and a total B abundance of 140 relative to  $10^6$  Si. However, the condensation of pure  $\text{NaBO}_2$  in the solar nebula is unlikely because B is a trace element and pure  $\text{NaBO}_2$  has not been observed in chondrites. In addition, at 750 K Na is completely condensed as albite in feldspar [12]. It is more plausible that B condenses into solid solution with major minerals.

For Be, Cameron et al. [13] used the total Be abundance of 0.81 reported by Sill and Willis [14] to calculate that Be completely condenses in solid solution with spinel at 1400 K. In another study, Spivack et al. [15] stated that Be would not be as refractory as Cameron et al. [13] predict. Instead, Spivack et al. [15] predict a Be condensation temperature in the range 980–1200 K. However, the details of their calculations are not published.

Table 1  
Boron and beryllium condensation temperatures

Temperature <sup>a</sup> (K)	Method	Reference
<b>Boron condensation temperatures</b>		
745–759 (100%)	Condensation as pure NaBO <sub>2</sub> , P <sub>T</sub> = 10 <sup>-3</sup> bar	[13]
1200	Relative boron abundance in mantle xenoliths	[16]
400–900	Correlation between boron and sulfur in chondrites	[20]
910 (50%)	Bulk B abundance and volatility trends for chondrites	[22]
964 (50%)	Condensation in feldspar solid solution, P <sub>T</sub> = 10 <sup>-3</sup> bar	This work
<b>Beryllium condensation temperatures</b>		
1400 (100%)	Condensation in spinel solid solution, P <sub>T</sub> = 10 <sup>-3</sup> bar	[13]
980–1250	Condensation as BeO	[15]
1490 (50%)	Condensation in melilite solid solution, P <sub>T</sub> = 10 <sup>-3</sup> bar	This work
1501 (50%)	Condensation in melilite and spinel solid solution, P <sub>T</sub> = 10 <sup>-3</sup> bar	This work

<sup>a</sup> Percentage refers to amount of element condensed at the stated temperature.

Since the work of Cameron et al. [13], there have been several other attempts to estimate the condensation temperature of B. Higgins and Shaw [16] measured the abundance of B in ultramafic xenoliths from alkali basalts thought to be representative of the Earth's upper mantle. Using CI-normalized B abundances they found that B is as depleted as Mn, Na and Ga and concluded that B has a condensation temperature similar to these elements, which they took as 1200 K at 10<sup>-4</sup> bar total pressure. However, the 50% condensation temperatures of Mn, Na, and Ga are 1190 K, 970 K, and 918 K (at 10<sup>-4</sup> bar), respectively [17], giving a 300° uncertainty in the B condensation temperature. Higgins and Shaw [16] conjectured that feldspar is the most likely B host phase at this temperature in the solar nebula.

Chaussidon and Jambon [18] measured the B content of oceanic basalt glasses as 0.25 ± 0.1 ppm, which they took as representative of the bulk silicate Earth. They report a B depletion factor relative to CI abundances of 0.15 and conclude that B is moderately volatile and condenses in low-temperature phases in the solar nebula. As a result, B should be concentrated in the matrix portion of chondrites, with the caveat that some B may be present in high-temperature phases such as Al-rich refractory inclusions. However, recent measurements show that the bulk B abundance in CI chondrites is 0.72 ± 0.07 ppm [19]. Using this value, the B depletion factor for the bulk silicate Earth is 0.35 ± 0.18.

Curtis and Gladney [20] measured the abundances of B, S, Si, and Na in 28 chondrites and used this

data to estimate the condensation temperature of B. Sulfur condenses at the pressure independent temperature of 713 K in the solar nebula [21] while Na is 50% condensed at 986 K (10<sup>-3</sup> bar). Curtis and Gladney [20] found a correlation between B and S but not between Na and B. They suggested that B is moderately volatile (like S) and should condense between 400 and 900 K.

Zhai and Shaw [19] present analyses of the B abundance in CI chondrites. They also found a correlation between B and S abundances but noted that the normalized abundance of B is usually higher than that of S. Zhai and Shaw [19] conclude that B has a higher condensation temperature than S and that the correlation between these two elements implies that both B and S abundances in carbonaceous chondrites result from a mixture of matrix and chondrule components. Zhai [22] used these data and the relationship between 50% condensation temperatures and CI-chondrite normalized elemental abundances in CM, CV, and CO chondrites [23] to estimate the condensation temperature of B from each meteorite class. The results of the three data sets gave 50% condensation temperatures for B in the range 880–930 K with an average value of 910 K.

### 3. Calculations

We calculated the condensation sequence of Be and B using an approach similar to that of Cameron et al. [13]. However, since then thermodynamic data

for Be and B gases have been revised and more thermodynamic data for B and Be gases and minerals are available. In addition, there are several recent studies of Be and B minerals that are relevant for understanding their condensation in solid solutions. Below we describe the mineral phases considered in our calculations, along with the sources of the thermodynamic data.

### 3.1. Mineralogy

As a first approximation, B and Be are expected to behave cosmochemically like other elements in their chemical groups of the periodic table. Thus, the condensation behavior of Be should be similar to that of Mg or Ca. Since Be is a trace element, it is unlikely that it will condense as a pure phase. Therefore, we considered solid solutions between known Be minerals and Mg- and Ca-bearing minerals condensing from a solar composition gas. Beryllium minerals analogous to akermanite ( $\text{Ca}_2\text{MgSi}_2\text{O}_7$ ), spinel ( $\text{MgAl}_2\text{O}_4$ ), and forsterite ( $\text{Mg}_2\text{SiO}_4$ ) are gugiaite ( $\text{Ca}_2\text{BeSi}_2\text{O}_7$ ), chrysoberyl ( $\text{BeAl}_2\text{O}_4$ ), and phenakite ( $\text{Be}_2\text{SiO}_4$ ), respectively.

Natural gugiaite was first discovered in skarn rocks near the village of Gugia, China [24]. Kimata [25] confirmed the suggestion of Gorja [26] that gugiaite is isostructural with akermanite. The crystal structure of gugiaite was refined by Kimata and Ohashi [27]. The various conditions under which gugiaite has been synthesized are presented in Table

2. Recently, Beckett et al. [28] measured the partition coefficient of Be between melilite and liquid. They found that Be was incompatible with gehlenitic melilite but compatible with akermanitic melilite.

Similarly, we compared the condensation behavior of B to that of Al. Phase diagrams indicate that there are several B compounds that form solid solutions with Al-bearing minerals. These are:  $\text{B}_2\text{O}_3$ ,  $\text{B}_2\text{Al}_4\text{O}_9$ , and  $\text{B}_4\text{Al}_{18}\text{O}_{33}$  in solution with corundum ( $\text{Al}_2\text{O}_3$ );  $\text{CaB}_2\text{O}_4$  and  $\text{CaB}_4\text{O}_7$  with hibonite ( $\text{CaAl}_{12}\text{O}_{19}$ ) or calcium dialuminate ( $\text{CaAl}_4\text{O}_7$ ); danburite ( $\text{CaB}_2\text{Si}_2\text{O}_8$ ) in solution with anorthite ( $\text{CaAl}_2\text{Si}_2\text{O}_8$ ); and reedmergnerite ( $\text{NaBSi}_3\text{O}_8$ ) in solution with albite ( $\text{NaAlSi}_3\text{O}_8$ ).

The mineral danburite is found in cavities and veins in igneous rocks as well as in association with ore deposits and salt deposits [29]. X-ray analyses of the crystal structure of danburite show that it is structurally similar to other feldspars, particularly anorthite [30].

Natural reedmergnerite has been found in the Green River Formation, Utah [31] and in a peralkaline pegmatite in Tajikistan [32]. Appleman and Clarke [33] reported that natural reedmergnerite is isostructural with low albite. Kimata [34] noted that an order–disorder transformation occurs at higher temperatures. Mason [35] found that the ordering behavior of reedmergnerite is similar to that of albite and Fleet [36] reported that the order–disorder transformation occurs in the 773–823 K temperature range at  $P_{\text{H}_2\text{O}} = 1$  kbar. Eugster and McIver [37] found that

Table 2  
Formation conditions of gugiaite and reedmergnerite

Starting materials	Temperature (K)	Pressure (kbar)	Reference
<b>Gugiaite (<math>\text{Ca}_2\text{BeSi}_2\text{O}_7</math>)</b>			
$\text{Ca}(\text{OH})_2$ , BeO, $\text{SiO}_2$	833	0.8	[25]
$\text{CaSiO}_3$ , BeO	1473	8.0	[27]
<b>Reedmergnerite (<math>\text{NaBSi}_3\text{O}_8</math>)</b>			
Not reported	573–773	2.0	[37]
Homogeneous glass	773, 973	2.0, 0.4	[56]
$\text{Na}_2\text{CO}_3$ , $\text{H}_3\text{BO}_3$ , $\text{SiO}_2$	543–623	0.10–0.42	[34]
$\text{Na}_2\text{CO}_3$ , $\text{B}_2\text{O}_3$ , $\text{SiO}_2$	573	0.10	[34]
$\text{NaOH}$ (6 N), $\text{B}_2\text{O}_3$ , $\text{SiO}_2$	573, 703	0.10, 0.39	[34]
$\text{NaOH}$ (6 N), $\text{H}_3\text{BO}_3$ , $\text{SiO}_2$	573, 703	0.10, 0.39	[34]
Silica gels	573, 673	1	[35]
$\text{NaBO}_2$ , $\text{SiO}_2$	735, 853	1.8, 0.8	[36]

Table 3  
Estimated thermodynamic data

Mineral	$C_p$ coefficients <sup>a</sup>					$S_{298}$ (J mol <sup>-1</sup> K <sup>-1</sup> )	$\Delta_f H_{298}$ (kJ mol <sup>-1</sup> )
	$c_1$	$c_2$	$c_3$	$c_4$	$c_5$		
Gugiaite (Ca <sub>2</sub> BeSi <sub>2</sub> O <sub>7</sub> )	94.2	16.5	-3.41	2.36	-6.60	165 ± 25	-3900 ± 600
Gugiaite (Ca <sub>2</sub> BeSi <sub>2</sub> O <sub>7</sub> ) <sup>b</sup>						167 ± 34	-3925 ± 800
Reedmergerite (NaBSi <sub>3</sub> O <sub>8</sub> )	572	-1.69	-1.64	-7.23	4.44	178 ± 27	-3687 ± 490

<sup>a</sup>  $C_p = c_1 + c_2 \times 10^{-2} T + c_3 \times 10^{-5} T^2 + c_4 \times 10^3 T^{-1/2} + c_5 \times 10^6 T^{-2}$  (J mol<sup>-1</sup> K<sup>-1</sup>).

<sup>b</sup> Derived from results of Beckett et al. [28].

an albite–reedmergerite solid solution exists and extends to Ab<sub>80</sub>Rd<sub>20</sub>. They also stated that the anhydrous melting temperature of reedmergerite is 1135 K. The conditions under which reedmergerite has been synthesized are also given in Table 2.

### 3.2. Thermodynamic data for Be and B minerals

Thermodynamic data for phenakite (Be<sub>2</sub>SiO<sub>4</sub>) and chrysoberyl (BeAl<sub>2</sub>O<sub>4</sub>) are well known [38]. Data for danburite were compiled from the results of several different research groups [39–43]. The data sets agree within stated uncertainties, with the exception of the value for the standard entropy ( $S_{298}^{\circ}$ ) of danburite. We choose the more recent value from Mazdab et al. [43]. For all other phases, with the exception of gugiaite and reedmergerite, the thermodynamic data sources are given in Fegley and Lodders [9].

The thermodynamic properties of gugiaite and reedmergerite are not known. However, by comparing gugiaite and reedmergerite to their isostructural Mg- and Al-bearing analogues (akermanite (Ak) and albite (Ab), respectively) and using standard techniques for estimating thermodynamic data [44] we estimated the heat capacity as a function of temperature ( $C_p$ ), the standard entropy ( $S_{298}^{\circ}$ ) and the heat of formation ( $\Delta H_{298}^{\circ}$ ). Our estimates are presented in Table 3. Also shown in Table 3 are values for  $S_{298}^{\circ}$  and  $\Delta H_{298}^{\circ}$  of gugiaite derived from the results of Beckett et al. [28]. They determined an entropy and enthalpy of reaction for the exchange of Be and Mg between liquid and melilite. The nominal values for  $S_{298}^{\circ}$  and  $\Delta H_{298}^{\circ}$  of gugiaite, derived from the results of Beckett et al. [28], agree with our estimated values, suggesting that our estimates are reasonable.

The heat capacity functions for gugiaite (Gu) and

reedmergerite (Rd) were estimated from the equations:

$$C_{p,Gu} = C_{p,Ak} - C_{p,MgO} + C_{p,BeO} \quad (1)$$

and:

$$C_{p,Rd} = C_{p,Ab} - \frac{1}{2} C_{p,Al_2O_3} + \frac{1}{2} C_{p,B_2O_3} \quad (2)$$

where  $C_{p,i}$  represents the heat capacity of phase *i* as a function of temperature.

The  $S_{298}^{\circ}$  values were estimated by comparing the standard entropies of minerals in which elements of

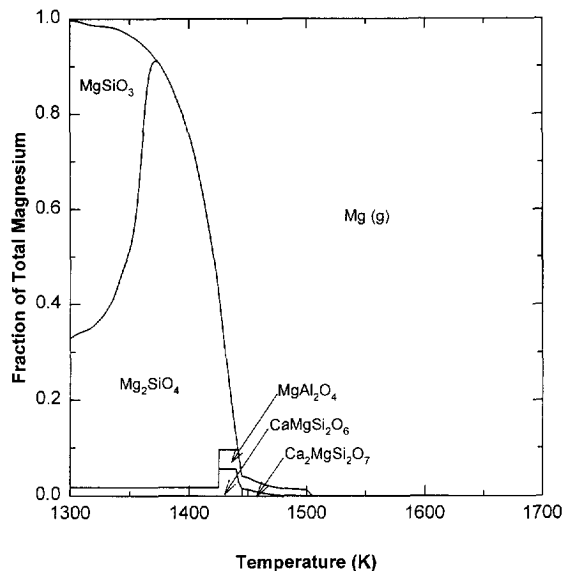


Fig. 1. Graph showing Mg chemistry at 10<sup>-3</sup> bar total pressure. The dominant gas is monatomic Mg at all temperatures displayed. The two main Mg-bearing solids are forsterite (Mg<sub>2</sub>SiO<sub>4</sub>) and enstatite (MgSiO<sub>3</sub>). Other Mg-bearing phases are akermanite (Ca<sub>2</sub>MgSi<sub>2</sub>O<sub>7</sub>), spinel (MgAl<sub>2</sub>O<sub>4</sub>), and diopside (CaMgSi<sub>2</sub>O<sub>6</sub>). Beryllium analogues of akermanite, spinel, and forsterite exist. Magnesium is 50% condensed at a temperature of 1420 K.

Table 4  
Condensation temperatures of pure boron and beryllium compounds at  $10^{-3}$  bar total pressure<sup>a</sup>

Boron compounds		Beryllium compounds	
Phase	T <sub>c</sub> (K)	Phase	T <sub>c</sub> (K)
CaB <sub>2</sub> Si <sub>2</sub> O <sub>8</sub>	1096	Ca <sub>2</sub> BeSi <sub>2</sub> O <sub>7</sub>	1344
B <sub>4</sub> Al <sub>18</sub> O <sub>33</sub>	1047	Be <sub>3</sub> B <sub>2</sub> O <sub>6</sub>	1256
NaBSi <sub>3</sub> O <sub>8</sub>	1003	BeAl <sub>2</sub> O <sub>4</sub>	1250
B <sub>2</sub> Al <sub>4</sub> O <sub>9</sub>	975	Be <sub>2</sub> SiO <sub>4</sub>	1020
CaB <sub>2</sub> O <sub>4</sub>	921	BeO	901
LiBO <sub>2</sub>	738		

<sup>a</sup> Assumes no prior condensation of B or Be-bearing phases.

the same chemical group can substitute, and which have similar crystal structures. For the group II elements we looked at the compounds XAl<sub>2</sub>O<sub>4</sub>, X<sub>2</sub>SiO<sub>4</sub>, X(OH)<sub>2</sub>, XSO<sub>4</sub>, and XWO<sub>4</sub>, where X represents Be, Mg, Ca, or Sr. The value of S<sub>298</sub><sup>0</sup> for Be-bearing minerals is approximately 0.6–0.8 times

that of the corresponding Mg compound. Similarly, for group III elements (B, Al, Ga and In) we compared the S<sub>298</sub><sup>0</sup> values for the following compounds: X<sub>2</sub>O<sub>3</sub>, X<sub>2</sub>S<sub>3</sub>, CaX<sub>2</sub>Si<sub>2</sub>O<sub>8</sub>, NaXO<sub>2</sub>, CaX<sub>2</sub>O<sub>4</sub>, and CaX<sub>4</sub>O<sub>7</sub>, where X represents a group III element. The value of S<sub>298</sub><sup>0</sup> for B-bearing minerals is 0.8–1.05 times that of the corresponding Al compound. We used these ranges to determine the mean and 1 sigma uncertainties for our estimated S<sub>298</sub><sup>0</sup> of gugiaite and reedmergnerite, which are given in Table 3.

The heat of formation was estimated from the free energy function ( $\Phi$ ) which was calculated from the standard entropy and the heat capacity via:

$$\Phi_{\text{Mineral}} = \frac{G_T - H_{298}^0}{T} = \frac{1}{T} \int_{298}^T C_p dT + \int_{298}^T \frac{C_p}{T} dT + S_{298}^0 \quad (3)$$

The free energy function is related to the Gibbs free energy of a mineral phase by the equation:

$$\Delta G_T^0 = (\Phi_{\text{Mineral}} - \sum \Phi_{\text{Elements}})T + \Delta H_{298}^0 \quad (4)$$

where  $\sum \Phi_{\text{Elements}}$  refers to the sum of the free energy

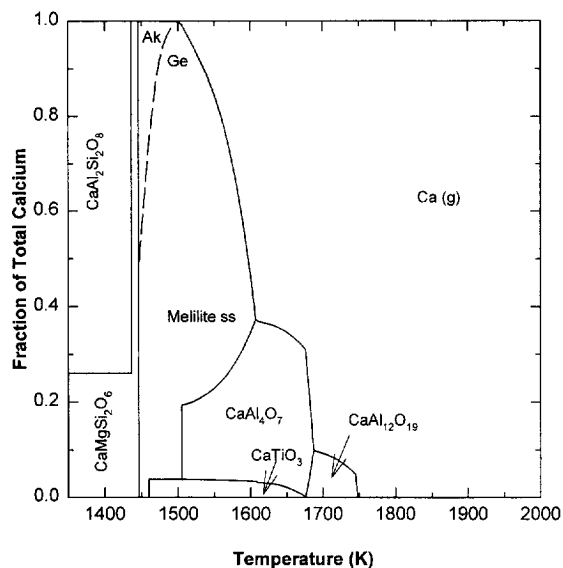


Fig. 2. Graph showing Ca chemistry at  $10^{-3}$  bar total pressure. The dominant gas is monatomic Ca at all temperatures displayed. The first Ca-bearing solid condensing is hibonite (CaAl<sub>12</sub>O<sub>19</sub>) followed by calcium dialuminate (CaAl<sub>4</sub>O<sub>7</sub>) and perovskite (CaTiO<sub>3</sub>). Most Ca is distributed among the melilite solid solution (Ca<sub>2</sub>Al<sub>2</sub>SiO<sub>7</sub>(Ge)–Ca<sub>2</sub>MgSi<sub>2</sub>O<sub>7</sub>(Ak)). The composition of this solution is shown as a dashed line on the graph. At the lowest temperatures shown Ca is distributed between anorthite (CaAl<sub>2</sub>Si<sub>2</sub>O<sub>8</sub>) and diopside (CaMgSi<sub>2</sub>O<sub>6</sub>). Calcium is 50% condensed at a temperature of 1615 K.

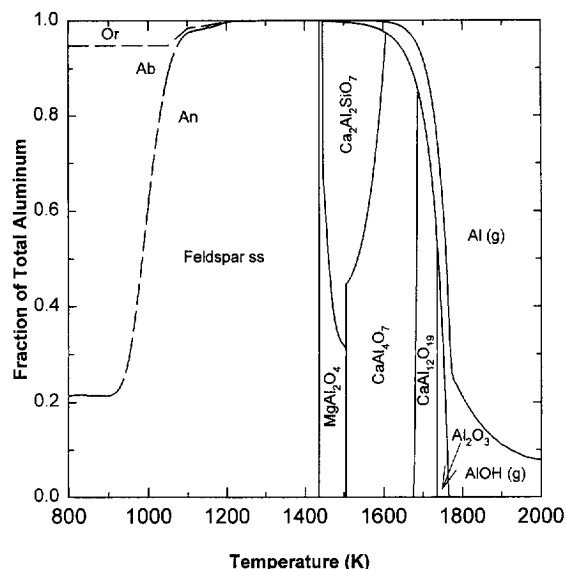


Fig. 3. Graph showing Al chemistry at  $10^{-3}$  bar total pressure. At lower temperatures Al is distributed among the three end-member feldspar system (Orthoclase (Or)–Albite (Ab)–Anorthite (An)). The composition of this solution is shown as a dashed line on the graph. B analogues of albite (NaAlSi<sub>3</sub>O<sub>8</sub>) and anorthite (CaAl<sub>2</sub>Si<sub>2</sub>O<sub>8</sub>) exist. Aluminum is 50% condensed at a temperature of 1735 K.

functions of the constituent elements in their respective reference states. The values of  $\Phi_{\text{Elements}}$  are from Robie and Hemingway [38]. Values for  $\Delta G_{\text{T}}^{\circ}$  were determined from known conditions of formation. If the  $\Delta G_{\text{T}}^{\circ}$  of all other compounds in the formation reaction are known, then an upper limit on the  $\Delta G_{\text{T}}^{\circ}$  (i.e., the least negative  $\Delta G_{\text{T}}^{\circ}$  value) is set by assuming that the net Gibbs free energy of the reaction is zero. This value can be substituted into Eq. (4) and an upper limit on  $\Delta H_{298}^{\circ}$  obtained.

For both gugiaite and reedmergnerite several different formation conditions are available (see Table 2), from which estimates of  $\Delta H_{298}^{\circ}$  can be obtained. Reedmergnerite was synthesized at 543 K but did not form at 523 K from identical starting materials [34]. The lowest temperature where reedmergnerite is stable is greater than 523 K but less than or equal to 543 K. This information constrains the heat of formation of reedmergnerite to within 20 kJ/mol. Similar information is not available for gugiaite and thus it is not possible to bracket a value of  $\Delta H_{298}^{\circ}$  for gugiaite. A value for  $\Delta H_{298}^{\circ}$  of gugiaite is derived

from each set of known formation conditions. We chose the minimum value obtained in this manner.

### 3.3. Condensation calculations

Once all of the thermodynamic data were compiled the condensation sequence of each element was calculated. The gas phase chemistry and major element distribution in pure phases was calculated using the CONDOR code, which uses the simultaneous constraints of mass balance and thermodynamic equilibrium to determine elemental distribution among an extensive library of gaseous and solid species. We used a total Be abundance of 0.73 [1] and a B abundance of 16.9 [22] relative to  $10^6$  atoms of Si. The Be and B gases included in our calculations and the data sources used are given in Fegley and Lodders [9]. The results for the major element distribution were then modified to consider the varying composition of solid solutions.

In order to determine which Be and B phases are likely to dissolve in major element host phases, the

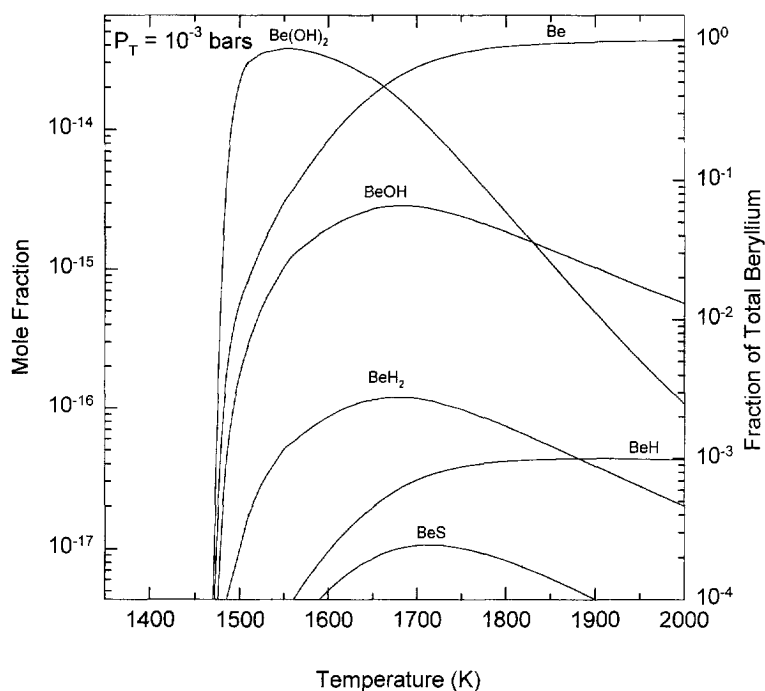


Fig. 4. Graph showing the distribution of Be among various gas phases at temperatures above the point where all Be is condensed. Abundances are shown as mole fractions relative to  $\text{H}_2 + \text{He}$  and as fraction of total Be. At high temperatures monatomic Be is dominant while the hydroxides ( $\text{BeOH}$  and  $\text{Be(OH)}_2$ ) become dominant at lower temperatures. Other Be gases are less abundant.

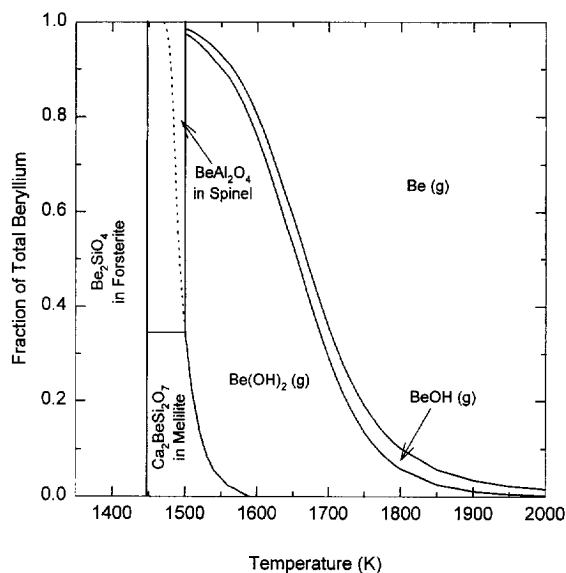


Fig. 5. Graph showing Be chemistry at  $10^{-3}$  bar total pressure. Be condenses in solid solution with melilite. Condensation in solid solution with spinel is also possible but the difference in the crystalline structures of spinel ( $\text{MgAl}_2\text{O}_4$ ) and chrysoberyl ( $\text{BeAl}_2\text{O}_4$ ) suggests that the solution will not be ideal. The dotted curve indicates the condensation of Be in melilite solid solution if condensation into spinel is ignored. The 50% condensation temperature of Be is 1501 K considering spinel and 1490 K without it. Uncertainties in the estimated thermodynamic data for Be melilite yield an uncertainty of  $\pm 30$  K in the Be 50% condensation temperature. Eventually all Be ends up as phenakite ( $\text{Be}_2\text{SiO}_4$ ) in forsterite.

condensation temperature of pure Be and B compounds were calculated. The condensation temperature is the temperature at which the activity of a solid equals unity. These temperatures were calculated using a total nebular pressure of  $10^{-3}$  bar and do not consider the previous condensation of any Be- or B-bearing phase. The pure phase condensation temperatures are given in Table 4.

The condensation temperature of a solid phase is increased by considering condensation in solid solution. Since Be most likely condenses into Mg- or Ca-bearing phases and B into Al-bearing phases, we calculated the condensation sequence of Mg, Ca, and Al (Fig. 1, Fig. 2, and Fig. 3, respectively). Our results agree well with previous condensation calculations [45,46]. Comparison of the condensation sequences for the major elements and the calculated condensation temperatures of pure Be and B miner-

als indicates that the most likely solid solutions are  $\text{Ca}_2\text{MgSi}_2\text{O}_7$ – $\text{Ca}_2\text{BeSi}_2\text{O}_7$ ,  $\text{MgAl}_2\text{O}_4$ – $\text{BeAl}_2\text{O}_4$ , and  $\text{Mg}_2\text{SiO}_4$ – $\text{Be}_2\text{SiO}_4$  for Be and  $\text{Al}_2\text{O}_3$ – $\text{B}_4\text{Al}_{18}\text{O}_{33}$ ,  $\text{CaAl}_2\text{Si}_2\text{O}_8$ – $\text{CaB}_2\text{Si}_2\text{O}_8$ , and  $\text{NaAlSi}_3\text{O}_8$ – $\text{NaBSi}_3\text{O}_8$  for B.

Fig. 4 shows the distribution of Be in the gas phase as a function of temperature. At higher temperatures Be exists mainly as monatomic Be gas while at lower temperatures the hydroxides  $\text{BeOH}$  and  $\text{Be(OH)}_2$  are more abundant.  $\text{BeH}$ ,  $\text{BeH}_2$ , and  $\text{BeS}$  account for less than 0.4% of all Be. Fig. 5 shows the condensation of Be into solid phases. Be condenses into melilite solid solution soon after melilite appears. If melilite is the only host phase then the 50% condensation temperature of Be is 1490 K and 100% of the Be is condensed into melilite at a temperature of 1470 K. These results are shown as the dashed curve in Fig. 5. The 50% condensation temperature of Be into melilite has an uncertainty of  $\pm 30$  K due to uncertainties in the estimated thermodynamic data. It is also possible that Be condenses into spinel. At the condensation temperature of spinel (1501 K)  $\sim 34\%$  of the Be is condensed into melilite. The activity of chrysoberyl ( $\text{BeAl}_2\text{O}_4$ ) at the point of spinel condensation is so large that, if the solid solution between chrysoberyl and spinel is ideal, all of the remaining Be condenses into this solid solution and the 50% condensation temperature of Be becomes equal to the condensation temperature of spinel (1501 K). The sequence for Be condensation into melilite and spinel is shown by the solid curves in Fig. 5. The spinel–chrysoberyl solid solution may be non-ideal since spinel and chrysoberyl are not isostructural. In fact, chrysoberyl has a crystal structure similar to that of forsterite [47]. In any case, the 50% condensation temperature

Table 5  
50% condensation temperatures of selected elements<sup>a</sup>

Element	Temperature (K)	Reference
Be	1490	This work
K	1064	This work
Na	986	This work
B	964	This work
S	674	[21]

<sup>a</sup>  $P_T = 10^{-3}$  bar.



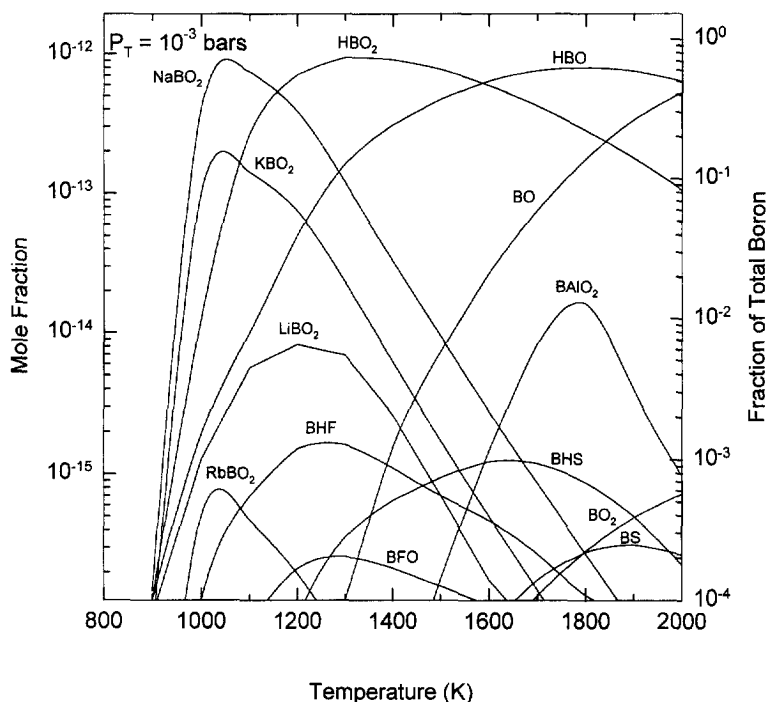


Fig. 6. Graph showing the distribution of B among various gases at temperatures above the point where all B is condensed. Abundances are shown as mole fractions relative to  $H_2 + He$  and as fraction of total B. At high temperatures HBO and BO are found to be the dominant species. At mid-range temperatures  $HBO_2$  becomes dominant. Eventually, alkali element-bearing species are the most abundant.

of Be is between 1490 and 1501 K at  $10^{-3}$  bar total pressure. Once forsterite is stable (1443 K) the activity of phenakite ( $Be_2SiO_4$ ) is very large, suggesting that, as melilite disappears from the nebula, all Be will go into forsterite.

Fig. 6 shows the distribution of B in the gas as a function of temperature. At higher temperatures, B exists as  $HBO_2(g)$ ,  $HBO(g)$ , and  $BO(g)$ . The gases  $NaBO_2$ ,  $KBO_2$ , and  $LiBO_2$  become increasingly abundant at lower temperatures. Fig. 7 shows the condensation behavior of B. Boron does not condense into solid solution with corundum, hibonite, or calcium dialuminate because the activities of the corresponding B compounds are insignificant. Instead, B starts to condense as danburite in solid solution with feldspar as soon as anorthite becomes stable (1436 K). This yields a B 50% condensation temperature of 964 K. At lower temperatures, where the feldspar composition is more albitic, B also condenses as reedmergnerite into feldspar. At the temperature where reedmergnerite condensation be-

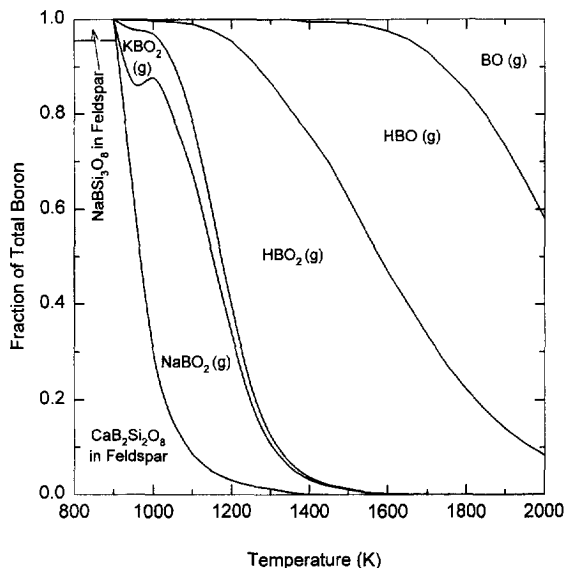


Fig. 7. Graph showing B chemistry at  $10^{-3}$  bar total pressure. Boron condenses in solid solution with feldspar, predominantly as danburite ( $CaB_2Si_2O_8$ ). The 50% condensation temperature of B is 964 K and 100% of B is condensed at 900 K.

comes significant ( $\sim 920$  K) more than 96% of B has already condensed as danburite. All of the B is condensed into solid solution with feldspar, either as danburite or reedmergerite at a temperature of 900 K. The 50% condensation temperatures of both B and Be at a total nebular pressure of  $10^{-3}$  bar are given in Table 1 and are compared to the 50% condensation temperatures of other elements in Table 5. According to our calculations, the 50% condensation temperature of B is close to that of Na (986 K) and well above that of S (674 K) [21]. This is in agreement with the findings of Higgins and Shaw [16], based on elemental abundances in mantle xenoliths.

#### 4. B and Be in meteorites

It is useful to compare the results of our calculations with previous measurements of Be and B abundances in meteorites. However, very little work has been done in measuring the Be and B content of individual mineral phases in meteorites. Most work has focused on the determination of Be and B bulk abundances [14,19,48]. Phinney et al. [49] measured B, Be, and Li abundances in Allende inclusion EK-1-07 but they reported that their B abundances may have been contaminated by laboratory materials. The largest Be concentration was in melilite (429 ppb) and smaller amounts of Be were found in anorthite (127 ppb) and pyroxene (177 ppb). An upper limit of 150 ppb was placed on the Be concentration of the spinel. Spivack et al. [15] also found Be concentrated in the melilite of several Allende CAIs. Similarly, MacPherson and Davis [50] measured Be abundances in a Vigarano type B CAI as 649 ppb in melilite, 204 ppb in fassaite, and 268 ppb in anorthite. These measurements show that the highest concentrations of Be are found in the melilite grains of CAIs and that meteoritic spinel does not contain large concentrations of Be. This suggests that Be is incompatible with spinel and that all Be initially condenses into melilite.

Shaw et al. [51] used alpha track images to locate B in meteorites. They found large concentrations of boron in the matrices of both carbonaceous and ordinary chondrites. However, specific B host phases were not identified. The only measurements of B

abundances in meteoritic minerals were made on a silicate inclusion, which has an H chondrite-like composition, from the Watson IIE iron meteorite [52]. The texture of the inclusion implies complete melting within the iron meteorite. The results of an ion probe study of trace element distribution among the various mineral phases of this inclusion show that the B concentration in the feldspar is 4–10 times higher than that in olivine, pyroxene, or whitlockite [52]. While this does not verify our conclusion that B condenses in solid solution with feldspar, it does illustrate the affinity of B for this mineral.

Chaussidon and Robert [53] measured B and Be abundances in olivine chondrules from the Semarkona, Hedjaz, and Allende chondrites. In the chondrules of all three of these meteorites they found a constant B/Be ratio of  $\sim 17.2$  and interpreted this as implying that there was no fractionation of B and Be during condensation in the solar nebula. However, the B/Be ratio in CI chondrites is 23.15 [1,19], indicating that some fractionation must have occurred to produce the two different ratios. Also, our results imply that there would be significant fractionation of B and Be during condensation from the cooling solar nebula. Fig. 8 shows the B/Be ratio against temperature inferred from our condensation calculations. Chaussidon and Robert [53] did not measure the composition of the melilite or feldspar phases of the meteorites they investigated so their results of a constant B/Be ratio may result from measurement of the composition of a single miner-

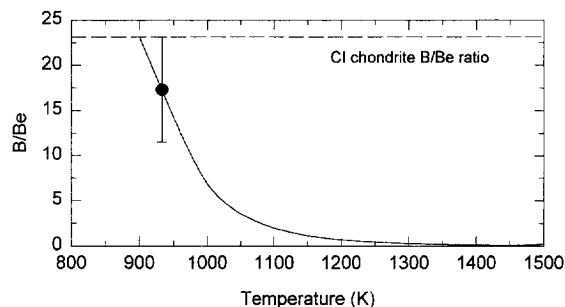


Fig. 8. Graph showing the B/Be ratio vs. temperature in the solar nebula. The B/Be ratio measured by Chaussidon and Robert [53] in olivine grains from various chondrites is shown as a black dot, along with their stated uncertainty. Our results indicate that significant fractionation will occur between these two elements at temperatures greater than 900 K.

alogical phase (olivine). We suggest examining other phases such as melilite and feldspar to determine if there was any fractionation of these two elements.

Finally, we discuss the B content of the bulk silicate earth since this value has been used to discuss B cosmochemistry [16,20,54]. Our calculations predict that the volatility of B is close to that of Na, which is depleted relative to CI chondrites in the bulk silicate earth by a factor of 0.6 [1,55]. The abundance of B in CI chondrites ranges from 0.65 to 0.78 ppm with an average value of 0.72 ppm [19]. A B depletion factor equal to that of Na implies an abundance of  $0.4 \pm 0.1$  ppm B in the bulk silicate earth. This value is between the B abundance of  $0.53 \pm 0.07$  ppm measured in mantle xenoliths thought to be representative of primitive mantle [16] and the value of  $0.25 \pm 0.1$  ppm derived from the B content of mid-ocean ridge basalts but is larger than the recent determination of  $0.10 \pm 0.02$  ppm based on the B content of ocean island basalts [54].

## 5. Summary

Condensation calculations for Be and B, whose abundances can constrain mechanisms responsible for the formation of light elements, are presented. In order to perform these calculations it was necessary to estimate thermodynamic data for two phases: gugiaite ( $\text{Ca}_2\text{BeSi}_2\text{O}_7$ ) and reedmergnerite ( $\text{NaBSi}_3\text{O}_8$ ). The condensation of Be and B was determined by considering solid solution in various mineral phases thought to be present in the solar nebula. Beryllium condenses in solid solution with melilite and possibly spinel. Ideal solid solution of gugiaite into melilite yields a 50% condensation temperature of 1490 K. Assuming that a chrysoberyl ideal solid solution with spinel also occurs, the 50% condensation temperature of Be increases to 1501 K. Once forsterite is stable, Be released by the consumption of melilite and spinel forms phenakite in solid solution with forsterite. Boron condenses in solid solution with feldspar. The 50% condensation temperature of B is 964 K, which is close to that of Na (986 K) and suggests that the abundance of these two elements in carbonaceous chondrites may be correlated. The few available measurements of the Be concentration in individual mineral phases in

meteorites find Be concentrated in melilite but not in spinel, supporting the assumption that the spinel–chrysoberyl solid solution is not ideal. Measurements of the B concentration of individual mineral grains in meteorites are rare but B has been found concentrated in the feldspars of a silicate inclusion in the Watson iron meteorite. This supports our conclusion that B has a strong affinity for feldspar and is likely to condense into solid solution with albite and anorthite in the solar nebula.

## Acknowledgements

This work was supported by NASA grant NAGW-3070. We thank B. Fegley, Jr. for initiating this research as a course project for D.S. Lauretta and for helpful discussions. We also thank M.K. Crombie for useful advice and A.G.W. Cameron, M. Chaussidon, and D. Shaw for constructive reviews. [UC]

## References

- [1] E. Anders and N. Grevesse, Abundances of the elements: Meteoritic and solar, *Geochim. Cosmochim. Acta* 53, 197–214, 1989.
- [2] E.M. Burbidge, G.R. Burbidge, W.A. Fowler and F. Hoyle, Synthesis of the elements in stars, *Rev. Mod. Phys.* 29, 547–650, 1957.
- [3] M. Meneguzzi, J. Audouze and H. Reeves, The production of the elements Li, Be, and B by galactic cosmic rays in space and its relation to stellar observation, *Astron. Astrophys.* 15, 337–359, 1971.
- [4] W.A. Fowler, G.R. Burbidge and E.M. Burbidge, Nuclear reactions and element synthesis in the surfaces of stars, *Astrophys. J. Suppl.* 17, 167–194, 1955.
- [5] T.P. Walker, G.J. Mathews and V.E. Viola, Astrophysical production rates for Li, Be, and B isotopes from energetic 1H and 4He reactions with HeCNO nuclei, *Astrophys. J.* 299, 745–751, 1985.
- [6] M. Casse, R. Lehoucq and E. Vangioni-Flam, Production and evolution of light elements in active star-forming regions, *Nature* 373, 318–319, 1995.
- [7] H. Reeves, W.A. Fowler and F. Hoyle, Galactic cosmic ray origin of Li, Be and B in stars, *Nature* 226, 727–729, 1970.
- [8] H. Reeves, On the origin of the light elements ( $Z < 6$ ), *Rev. Mod. Phys.* 66, 193–216, 1994.
- [9] B. Fegley Jr. and K. Lodders, Chemical models of the deep atmospheres of Jupiter and Saturn, *Icarus* 110, 117–154, 1994.

- [10] H.B. Niemann, S.K. Atreya, G.R. Carignan, T.M. Donahue, J.A. Haberman, D.N. Harpold, R.E. Hartle, D.M. Hunten, W.T. Kasprzak, P.R. Mahaffy, T.C. Owen, N.W. Spencer and S.H. Way, The Galileo Probe Mass Spectrometer: Composition of Jupiter's atmosphere, *Science* 272, 846–849, 1996.
- [11] D.M. Shaw, M.D. Higgins, M.G. Truscott and T.A. Middleton, Boron contamination in polished thin sections of meteorites: Implications for other trace-element studies by alpha-track image or ion microprobe, *Am. Mineral.* 73, 894–900, 1988.
- [12] C.M. Wai and J.T. Wasson, Nebular condensation of moderately volatile elements and their abundances in ordinary chondrites, *Earth Planet. Sci. Lett.* 36, 1–13, 1977.
- [13] A.G.W. Cameron, S.A. Colgate and L. Grossman, Cosmic abundance of boron, *Nature* 243, 204–207, 1973.
- [14] C.W. Sill and C.P. Willis, The beryllium content of some meteorites, *Geochim. Cosmochim. Acta* 26, 1209–1214, 1962.
- [15] A.J. Spivack, H. Gnaser, J.R. Beckett, C.I. Measures, I.D. Hutcheon and J.G. Wasserburg, The abundance and distribution of Be in Allende inclusions, *Lunar Planet. Sci. Conf.* 18, 938–939, 1987.
- [16] M.D. Higgins and D.M. Shaw, Boron cosmochemistry interpreted from abundances in mantle xenoliths, *Nature* 308, 172–173, 1984.
- [17] B. Fegley Jr., Chemistry of the Solar Nebula, in: *The Chemistry of Life's Origins*, M. Greenberg, C.X. Mendoza-Gomez and V. Pirronello, eds., NATO Adv. Sci. Inst. C 416, pp. 75–147, Kluwer, Dordrecht, 1993.
- [18] M. Chaussidon and A. Jambon, Boron content and isotopic composition of oceanic basalts: Geochemical and cosmochemical implications, *Earth Planet. Sci. Lett.* 121, 277–291, 1994.
- [19] M. Zhai and D. Shaw, Boron cosmochemistry. Part I: Boron in meteorites, *Meteoritics* 29, 607–615, 1994.
- [20] D.B. Curtis and E.S. Gladney, Boron cosmochemistry, *Earth Planet. Sci. Lett.* 75, 311–320, 1985.
- [21] D.S. Lauretta, D.K. Kremser and B. Fegley Jr., The rate of iron sulfide formation in the solar nebula, *Icarus* 122, 288–315, 1996.
- [22] M. Zhai, Boron cosmochemistry. Part II: Boron nucleosynthesis and condensation temperature, *Meteoritics* 30, 733–735, 1995.
- [23] J.T. Wasson and G.W. Kallemeyn, Compositions of chondrites, *Philos. Trans. R. Soc. London A* 325, 535–544, 1988.
- [24] P. Chi-jui, T. Rung-lung and Z. Zu-rung, Gugiaite,  $\text{Ca}_2\text{BeSi}_2\text{O}_7$ , a new beryllium mineral and its relation to the melilite group, *Sci. Sinica* 11, 977–988, 1962.
- [25] M. Kimata, Crystal chemistry of Ca-melilites on X-ray diffraction and infrared absorption properties, *Neues Jahrb. Mineral. Abh.* 139, 43–58, 1980.
- [26] C. Gorla, Struttura della berillio-akermanite, *Atti Accad. Sci. Torino Cl. Sci. Fis. Mat. Nat.* 88, 153–160, 1954.
- [27] M. Kimata and H. Ohashi, The crystal structure of synthetic gugiaite,  $\text{Ca}_2\text{BeSi}_2\text{O}_7$ , *Neues Jahrb. Mineral. Abh.* 143, 210–222, 1982.
- [28] J.R. Beckett, A.J. Spivack, I.D. Hutcheon, G.J. Wasserburg and E.M. Stolper, Crystal chemical effects on the partitioning of trace elements between mineral and melt: An experimental study of melilite with applications to refractory inclusions from carbonaceous chondrites, *Geochim. Cosmochim. Acta* 54, 1755–1774, 1990.
- [29] H.P. Eugster and W.S. Wise, Synthesis and stability of danburite and datolite, *Schweiz. Mineral. Petrogr. Mitt.* 43, 135–152, 1964.
- [30] M.W. Phillips, G.V. Gibbs and P.H. Ribbe, The crystal structure of danburite: A comparison with anorthite, albite, and reedmergnerite, *Am. Mineral.* 59, 79–85, 1974.
- [31] C. Milton, E.C.T. Chao, J.M. Axelrod and F.S. Grimaldi, Reedmergnerite,  $\text{NaBSi}_3\text{O}_8$ , the boron analogue of albite, from the Green River formation, Utah, *Am. Mineral.* 45, 188–199, 1960.
- [32] E.S. Grew, D.I. Belakovskiy, M.E. Fleet, M.G. Yates, J.J. McGee and N. Marquez, Reedmergnerite and associated minerals from peralkaline pegmatite, Dara-i-Pioz, southern Tien Shan, Tajikistan, *Eur. J. Mineral.* 5, 971–984, 1993.
- [33] D.E. Appleman and J.R. Clark, Crystal structure of reedmergnerite, a boron albite, and its relation to feldspar crystal chemistry, *Am. Mineral.* 50, 1827–1850, 1965.
- [34] M. Kimata, Synthesis and properties of reedmergnerite, *J. Japan Assoc. Mineral. Petrol. Econ. Geol.* 72, 162–172, 1977.
- [35] R.A. Mason, The ordering behavior of reedmergnerite,  $\text{NaBSi}_3\text{O}_8$ , *Contrib. Mineral. Petrol.* 72, 329–333, 1980.
- [36] M.E. Fleet, Tetrahedral-site occupancies in reedmergnerite and synthetic boron albite ( $\text{NaBSi}_3\text{O}_8$ ), *Am. Mineral.* 77, 76–84, 1992.
- [37] H.P. Eugster and N.L. McIver, Boron analogous of alkali feldspars and related silicates, *GSA Bull.* 70, 1598–1599, 1959.
- [38] R.A. Robie and B.S. Hemingway, Thermodynamic properties of minerals and related substances at 298.15 K and 1 bar ( $10^5$  Pascals) pressure and at higher temperatures, *US Geol. Surv. Bull.* 2131, 1995.
- [39] V.M. Agoshkov, Yu.V. Semenov, S.V. Malinko and I.L. Khodakovskiy, Enthalpies of datolite and danburite between 298.15 and 973.15 K, *Geochem. Int.* 14, 142–147, 1977.
- [40] V.M. Zhdanov, V.A. Turdakin, V.S. Arutyunov, Yu.V. Semenov, S.V. Malinko and I.L. Khodakovskiy, Low-temperature specific heat, standard entropy, and elastic parameters of datolite and danburite, *Geochem. Int.* 14, 135–141, 1977.
- [41] Yu.V. Semenov, S.V. Malinko, I.A. Kiseleva and I.L. Khodakovskiy, The formation conditions of endogenous calcium borates and borosilicates, *Geochem. Int.* 25, 103–111, 1988.
- [42] F.K. Mazdab, L.M. Anovitz, B.S. Hemingway, R.A. Robie and A. Navrotsky, Thermodynamic properties of some boron-bearing minerals, *GSA Abstr. Prog.* 24, 258, 1992.
- [43] F.K. Mazdab and L.M. Anovitz, New borate and borosilicate thermodynamic data, and an overview of boron mineral assemblages, *GSA Abstr. Prog.* 26, A-448, 1994.
- [44] O. Kubaschewski, C.B. Alcock and P.J. Spencer, *Materials Thermochemistry*, 6th ed., 363 pp., Pergamon, New York, NY, 1993.

- [45] S.K. Saxena and G. Eriksson, Chemistry of the formation of the terrestrial planets, in: *Chemistry and Physics of Terrestrial Planets*, S.K. Saxena, ed., Springer, New York, NY, 1986.
- [46] S. Yoneda and L. Grossman, Condensation of CaO–MgO–Al<sub>2</sub>O<sub>3</sub>–SiO<sub>2</sub> liquids from cosmic gases, *Geochim. Cosmochim. Acta* 59, 3413–3444, 1995.
- [47] E.F. Farrell, J.H. Fang and R.E. Newnham, Refinement of the chrysoberyl structure, *Am. Mineral.* 48, 804–810, 1963.
- [48] D.B. Curtis, E.S. Gladney, and E. Jurney, A revision of the meteorite based cosmic abundance of boron, *Geochim. Cosmochim. Acta* 44, 1945–1953, 1980.
- [49] D. Phinney, B. Whitehead and D. Anderson, Li, Be, and B in minerals of a refractory-rich Allende inclusion, *Proc. Lunar Planet. Sci. Conf.* 10, 885–905, 1979.
- [50] G.J. MacPherson and A.M. Davis, A petrologic and ion microprobe study of a Vigarano Type B refractory inclusion: Evolution by multiple stage of alteration and melting, *Geochim. Cosmochim. Acta* 57, 231–243, 1993.
- [51] D.M. Shaw, M.D. Higgins, R.W. Hinton, M.G. Truscott and T.A. Middleton, Boron in chondritic meteorites, *Geochim. Cosmochim. Acta* 52, 2311–2319, 1988.
- [52] E. Olsen, A. Davis, R.S. Clarke Jr., L. Schultz, H.W. Weber, R. Clayton, T. Mayeda, E. Jarosewich, P. Sylvester, L. Grossman, M. Wang, M.E. Lipschutz, I.M. Steele and J. Schwade, Watson: A new link in the IIE iron chain, *Meteoritics* 29, 200–213, 1994.
- [53] M. Chaussidon and F. Robert, Nucleosynthesis of 11B-rich boron in the pre-solar cloud recorded in chondrules, *Nature* 374, 337–339, 1995.
- [54] M. Chaussidon and B. Marty, Primitive boron isotope composition of the mantle, *Science* 269, 383–386, 1995.
- [55] J.S. Kargel and J.S. Lewis, The composition and early evolution of the earth, *Icarus* 105, 1–25, 1993.
- [56] E. Bruno and H. Pentinghaus, Substitution of cations in natural and synthetic feldspars, in: *The Feldspars*, Proc. NATO Adv. Study Inst., Manchester July 11–21 1972, W.S. MacKenzie and J. Zussman, eds., pp. 574–609, 1974.